

## Intercalation of silver in titanium disulfide

D. Kaluarachchi\* and R. F. Frindt

*Department of Physics, Simon Fraser University, Burnaby, British Columbia, Canada V5A 1S6*

(Received 10 September 1984)

The motion of Ag in partially intercalated  $\text{TiS}_2$  crystals has been studied using electron microprobe x-ray fluorescence and radioactive  $^{110}\text{Ag}$ . For high intercalation rates, a stage-2 Ag region is observed along with a stage-1 Ag region near the edge of the crystal. For low intercalation rates, no stage-1 region is observed. If the intercalation is stopped, the stage-1 Ag rapidly converts into stage-2. The stage-2 front then remains stationary at room temperature. Above  $100^\circ\text{C}$  the stage-2 front starts to penetrate the empty crystal. The  $^{110}\text{Ag}$  tracer results show that as Ag atoms enter the crystal edge, the preintercalated Ag is driven further into the crystal. Also during stage conversion the Ag from stage-1 drives the stage-2 Ag further into the crystal. Deintercalation of a stage-1 crystal proceeds by the propagation of a stage-2 front in from the crystal edge. A moving-island model for stage-2 is required to explain the intercalation, deintercalation, and stage-conversion results. The diffusion constant for Ag perpendicular to the  $\text{TiS}_2$  layers is shown to be negligible at room temperature ( $< 10^{-15}$   $\text{cm}^2/\text{sec}$ ) and about  $10^{-13}$   $\text{cm}^2/\text{sec}$  at  $200^\circ\text{C}$ .

### I. INTRODUCTION

Structural studies on intercalated layered systems have shown that intercalation generally occurs in stages.<sup>1</sup> By staging we mean that the intercalated species occupies the space between the host layers in an ordered sequence, where the stage number  $n$  refers to the number of host layers between the intercalant layers. In the so-called classical model of staging, layers between the host structure are entirely occupied by the guest atoms while some layers are completely empty. This model has difficulty in explaining the formation of higher stages by a simple rearrangement of the guest atoms within a given layer and requires motion of intercalant perpendicular to the layers. In the Daumas-Hérol (DH) model of staging,<sup>2</sup> the guest atoms are found in all the layers between the host structure and regular islands of guest atoms are arranged in a manner to form the different stages. Although the DH model provides the most plausible explanation for stage conversion, the model has not been directly verified.

In earlier work<sup>3,4</sup> it was shown that when Ag is rapidly electrointercalated into  $\text{TiS}_2$ , first a stage-2 region with  $x = 0.2$  (in the formula  $\text{Ag}_x\text{TiS}_2$ , where  $x$  is the local Ag concentration) is seen to propagate into the  $\text{TiS}_2$  from the edge of the crystal, followed by a stage-1 region with  $x = 0.4$ . If the intercalation is stopped before the crystal is fully intercalated, a conversion of the stage-1 region into stage-2 is observed. In this paper we present a detailed account of the stage-1 to stage-2 conversion, at room temperature and at elevated temperatures using electron microprobe x-ray fluorescence (XRF). In addition, the motion of the Ag in  $\text{TiS}_2$  crystals during slow (only stage-2 observed) intercalation and during stage-1 to stage-2 conversion has been monitored with radioactive  $^{110}\text{Ag}$ . It is found that Ag motion can only be reasonably explained using a DH type of model.

The motion of intercalated atoms in layered structures is generally regarded as "two dimensional"; however, little

data on this is available. The one study we have found for layered systems is for  $\text{Bi}_2\text{Te}_3$ , where the diffusivity parallel to the layers is about eight orders of magnitude greater than that in the direction perpendicular to the layers.<sup>5</sup> We present here data on the motion of Ag perpendicular to the layers of  $\text{TiS}_2$ . The results justify the two-dimensional assumption at room temperature.

### II. EXPERIMENTAL PROCEDURE AND RESULTS

#### A. Motion of Ag along the layers of $\text{TiS}_2$ at various temperatures

Pure  $\text{TiS}_2$  crystals were prepared by the iodine-vapor-transport method and the crystals used for intercalation were obtained by cleaving the as-grown crystals. For XRF measurements the thicknesses of the crystals used were in the range  $1\text{--}2\ \mu\text{m}$  and the lateral dimensions of the crystals were usually less than  $1000\ \mu\text{m}$ . The cleaved crystals were mounted on pieces of cover glass and the thicknesses were measured using optical interference fringes. Using a solution of  $0.1\text{M}$   $\text{AgNO}_3$  in glycerol, an open-circuit potential of  $200\ \text{mV}$  is observed and crystals can be electrointercalated by completing the external cell circuit. The crystals were allowed to electrointercalate partially only from one edge by covering the other edges with silicone rubber. The relative intercalated Ag content as a function of distance in from the crystal edge was determined by counting electron-beam-stimulated fluorescent x-ray emission in a scanning electron microprobe, using scans along a line perpendicular to the edge of the crystal. The accelerating voltage of the electron beam was  $20\ \text{kV}$ . The x-rays were analyzed by an energy-dispersive spectrometer and the x-ray intensity of the  $\text{Ag } L\alpha$  peak was measured relative to the intensity of the  $\text{Ti } K\alpha$  peak using a window width of  $0.3\ \text{keV}$ . The scans were point measurements taken about  $5$  to  $20\ \mu\text{m}$  apart and the electron-beam spot size was typically about  $2\ \mu\text{m}$  across.

The counting time per point was typically about 3 min. A typical XRF result is shown in Fig. 1.

To study the motion of Ag after partial intercalation, repeated XRF scans were carried out, and Fig. 2 shows a series of scans taken at room temperature. It is seen that the Ag in the stage-1 region disappeared rapidly within hours while the stage-2 region increased in size. It is clear from the areas under the stage-1 and stage-2 curves that the stage-1 Ag is converted into stage-2 and that the concentration in the occupied layers is essentially the same for both stages. It is of interest to note from Fig. 2 that the displacement of the stage fronts is initially linear in time ( $\sim 5 \mu\text{m}/\text{h}$ ). After a sufficient time, only stage-2 Ag was found in the crystal. After the stage-1 to stage-2 conversion is completed, the crystal was further studied to observe the motion of the stage-2 Ag, but no subsequent motion was found over a period of two months at room temperature. It is clear that in the absence of stage-1, the interface between stage-2 and empty crystal remains stationary at room temperature.

The crystals with only stage-2 regions were subsequently heated in an argon atmosphere and the distribution of Ag was determined after each heating by XRF scans at room temperature (Fig. 3). The distribution of Ag was not changed significantly by temperatures lower than  $100^\circ\text{C}$ ; however, as the temperature is increased, the Ag front advances into the empty crystal and the entire original stage-2 region loses some Ag, converting the intercalated region to a lower average Ag composition. At a sufficiently high temperature the Ag was distributed throughout the crystal. The peaks and valleys obtained in the final graph suggests a separation of phases, possibly a stage-2 and a "dilute" stage-1 phase.

Although the stage-1 Ag converts rapidly into stage-2 at room temperature (Fig. 2), both the stage-1 and stage-2 fronts remained stationary at liquid- $\text{N}_2$  temperature as shown by experiments where some crystals with both stages were left in liquid nitrogen for about a day. Monitoring the stage front positions by optical reflection (the intercalated regions are less reflecting) indicated that the Ag in both stages had not moved at 77 K.

We have observed that it is possible to partially deintercalate stage-1 crystals by applying a reverse potential greater than  $\sim 50 \text{ mV}$ . The deintercalation of  $\text{Ag-TiS}_2$

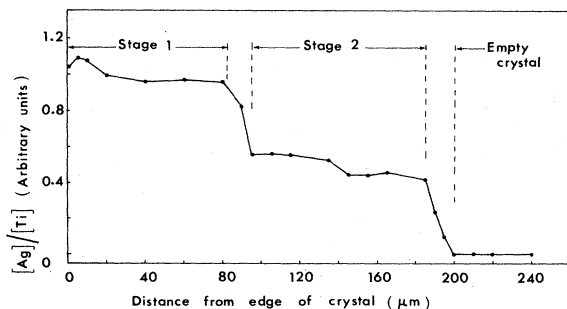


FIG. 1. X-ray fluorescence trace showing the distribution of Ag in a partially intercalated  $\text{TiS}_2$  crystal.

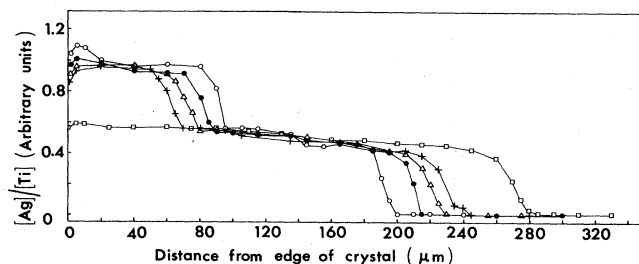


FIG. 2. Motion of Ag in a partially intercalated  $\text{TiS}_2$  crystal at room temperature. Time after intercalation: (a)  $\circ$ —45 min, (b)  $\bullet$ —2.75 h, (c)  $\triangle$ —4.25 h, (d)  $+$ —6.5 h, (e)  $\square$ —2 d.

crystal also occurs in stages. When a crystal in stage-1 deintercalates, the edge region first starts to convert to stage-2 from the stage-1 and then the depleted region proceeds further into the crystal (Fig. 4). As for intercalation, the density of Ag in the deintercalated stage-2 region is half of that of the stage-1 region. We have found that it was not possible to deintercalate crystals below stage-2 using glycerol or water electrolytes at room temperature.

### B. Tracer experiments

One of the interesting questions to be answered regarding intercalation of Ag in  $\text{TiS}_2$  is where the Ag atoms go after entering a partially intercalated stage-2 crystal. The possible answers are (i) the entering Ag atoms push the preintercalated Ag atoms further into the crystal and remain near the edge, (ii) the entering Ag atoms advance to the stage-2 front by moving past the preintercalated atoms, or (iii) some combination of (i) and (ii). A second question concerns the migration of Ag from the stage-1 region during the stage-1 to stage-2 conversion. Here the possible ways for redistribution from stage-1 Ag are (i) half of the Ag in the stage-1 region advances to the stage-2 front, (ii) the Ag in stage 1 pushes the existing stage-2 Ag into the empty region of the crystal, or (iii) some combination of (i) and (ii). In an attempt to answer these questions, experiments were carried out using radioactive  $^{110}\text{Ag}$  which has a half-life of 253 d. The activity associated with the whole gamma spectrum (energy  $\geq 100 \text{ keV}$ ) from the  $^{110}\text{Ag}$  was detected with a NaI well-type scintil-

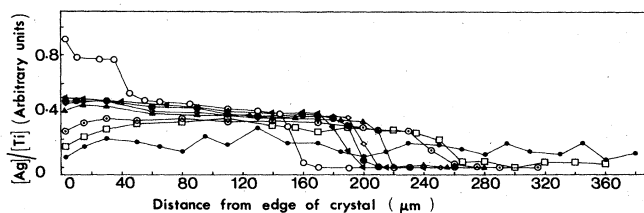


FIG. 3. Temperature dependence of motion of stage-2 Ag in  $\text{TiS}_2$ . (a)  $\circ$ —room temperature, 1 h after intercalation. (b)  $\triangle$ —room temperature, after all stage-1 is converted into stage-2. After consecutive heating for 2 h at increasing temperature: (c)  $\otimes$ — $100^\circ\text{C}$ , (d)  $\diamond$ — $150^\circ\text{C}$ , (e)  $\blacktriangle$ — $200^\circ\text{C}$ , (f)  $\odot$ — $275^\circ\text{C}$ , (g)  $\square$ — $300^\circ\text{C}$ , (h)  $\bullet$ — $325^\circ\text{C}$ .

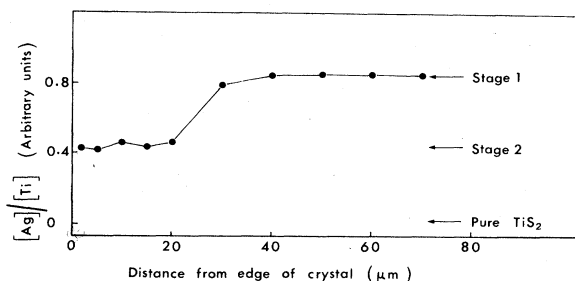


FIG. 4. Distribution of Ag in a partially deintercalated  $\text{TiS}_2$  crystal (the crystal thickness was between 0.5 and 1.0  $\mu\text{m}$ ).

lation spectrometer. The thickness of  $\text{TiS}_2$  crystals used in the tracer experiments ranged from 3 to 6  $\mu\text{m}$ . The crystals were peeled from as-grown crystals and it was very important to use crystals without cracks, pinholes, steps, scratches, or other macroscopic defects because intercalation is possible at these defects. The crystals were mounted on a piece of glass and a very small piece of Ag was attached to the crystal with a graphite dag to make a short-circuited cell. An electrolyte container was made using a small rubber *O* ring. Since a radioactive electrolyte was used, a minimum amount of the electrolyte (about 55  $\mu\text{l}$ ) was used.

### 1. Stage-2 intercalation

To study how the Ag atoms move in a stage-2 crystal while it is being intercalated, radioactive  $^{110}\text{Ag}$  was used to label the new guest atoms. The crystals were partially intercalated such that only stage-2 was obtained (it is possible to obtain only a stage-2 region in a crystal by limiting the intercalation rate using a low electrolyte concentration). A solution of 0.001M  $^{110}\text{Ag}$  in 0.05M  $\text{HNO}_3$  in water ( $^{110}\text{Ag}$  was only available in a  $\text{HNO}_3$  solution) was used as the active electrolyte and the nonactive electrolyte was made up with the identical molarity and solvent as the active one.

A crystal was first intercalated with nonactive  $^{108}\text{Ag}$  until the stage-2 front moved a distance  $y_1$  (Fig. 5), typically about 60 to 100  $\mu\text{m}$  from the crystal edges. Next, the crystal was again intercalated using the active electrolyte until the stage-2 front progressed a further distance typically about 30 to 40  $\mu\text{m}$  into the crystal giving a total stage-2 width of  $y_2$ . An optical reflection microscope was used to measure the widths  $y_1$  since the intercalated region is less reflecting than the empty region. The width of the active Ag region ( $y_2 - y_1$ ) was calculated from the

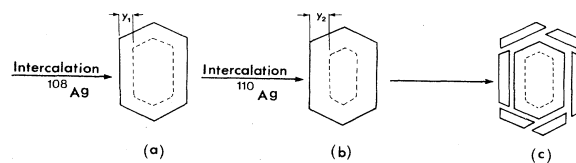


FIG. 5. Sequence of intercalation of a crystal and cutting the edges for tracer experiments. Dashed line depicts Ag intercalation front. (a)  $y_1$  is the width of stage-2  $^{108}\text{Ag}$ . (b)  $y_2$  is the width of stage-2 made up of  $^{108}\text{Ag}$  and  $^{110}\text{Ag}$ . (c) The widths of the cutoff sections and the width of the stage-2 region in the remaining part of the crystal are slightly greater than the active region ( $y_2 - y_1$ ).

values of  $y_1$  and  $y_2$  since the boundary of the active and nonactive regions could not be observed optically. The crystals were intercalated such that  $y_1 > y_2 - y_1$ . Then  $y_2 > 2(y_2 - y_1)$  and therefore it was possible to cut off the edges of the crystal such that the widths of the cut sections and the width of the stage-2 region in the remaining part of the crystal are slightly greater than the width of the active region ( $y_2 - y_1$ ). To determine the distribution of the active  $^{110}\text{Ag}$  in the crystal, the total crystal activity was first measured and then narrow sections of the crystal edges were cut with a razor blade as shown in Fig. 5(c). This was done under an optical microscope. After cutting, the activity of all the cut sections and the activity of the remaining part of the crystal were measured separately. If the new guest atoms ( $^{110}\text{Ag}$ ) remain near the edge regions of the crystal, the total activity of the edge regions should be equal to the initial activity of the uncut crystal. The results in Table I clearly show that most of the active Ag atoms remained in the edge region. A low but not negligible activity was found in the inner part, indicating some penetration of active Ag into the nonactive regions.

### 2. Stage-1 to stage-2 conversion

To study the motion of Ag from the stage-1 region during the stage-1 to stage-2 conversion,  $^{110}\text{Ag}$  was used to label the stage-1 Ag. The nonactive electrolyte used was a solution of 0.01M  $^{108}\text{Ag}$  in 0.05M  $\text{HNO}_3$  solution and the active electrolyte was a mixture of  $^{110}\text{Ag}$  and  $^{108}\text{Ag}$  with the same molarity and solvent as the nonactive one [a concentrated electrolyte (0.01M) was needed to obtain a stage-1 region]. Since the high concentration increased the radioactivity,  $^{110}\text{Ag}$  solution was mixed with nonactive  $^{108}\text{Ag}$  to reduce the activity to an acceptable level. Our XRF results showed that when a stage-1 region is converted to the stage-2 region, the additional width of

TABLE I. Results of  $^{110}\text{Ag}$  tracer experiments: Motion of Ag in stage-2 intercalation.  $y_2 - y_1$  is the width of the active  $^{110}\text{Ag}$  region.

Sample no.	Thickness ( $\pm 0.1 \mu\text{m}$ )	$y_1$ ( $\pm 5 \mu\text{m}$ ) $^{108}\text{Ag}$	$y_2$ ( $\pm 5 \mu\text{m}$ ) $^{108}\text{Ag} + ^{110}\text{Ag}$	$(y_2 - y_1)$ $^{110}\text{Ag}$	Width of cut sections ( $\pm 10 \mu\text{m}$ )	Counts per second		
						Whole crystal	Cut sections	Remaining crystal
1	6.0	60	90	30	40	9.62 $\pm$ 0.23	8.14 $\pm$ 0.22	1.38 $\pm$ 0.18
2	5.8	80	110	30	40	9.13 $\pm$ 0.23	7.92 $\pm$ 0.22	1.23 $\pm$ 0.18

the stage-2 region obtained by the stage conversion is equal to the width of the stage-1 region (Fig. 2). Therefore the crystals in this experiment were intercalated such that the width of the stage-2 ( $^{108}\text{Ag}$ ) region ( $z_1$ ) was greater than twice the width of stage-1 ( $^{110}\text{Ag}$ ) region ( $z_2$ ). Therefore  $z_1$  is greater than the width of the stage-2 region generated by the stage-1 to stage-2 conversion ( $2z_2$ ). To satisfy this condition, a crystal was preintercalated with  $^{108}\text{Ag}$  so that a wide band of stage-2  $^{108}\text{Ag}$  was obtained. Intercalation with nonactive  $^{108}\text{Ag}$  was then continued until a stage-1 front was just observed (by optical reflection) at the edge and then the electrolyte was quickly changed to the active  $^{110}\text{Ag}$  solution. This procedure ensured that active  $^{110}\text{Ag}$  atoms were intercalated only as stage-1. Intercalation with  $^{110}\text{Ag}$  was continued until the width of stage-1 region ( $z_2$ ) was typically 30 to 50  $\mu\text{m}$ . The width of the stage-2  $^{108}\text{Ag}$  region ( $z_1$ ) obtained was typically about 100 to 130  $\mu\text{m}$ . After the intercalation, the crystal was left for about a day to allow the stage-1  $^{110}\text{Ag}$  to convert into stage-2. At this point the total crystal activity was measured. The edge regions were then cut at a little more than  $2z_2$  from the edges. The activity in the cut sections and in the remaining part of the crystal was measured separately. If the  $^{110}\text{Ag}$  from stage-1 remained in a region adjacent to the edge of the crystal, then the total crystal activity of the edge region should be equal to the activity of the uncut crystal. The results given in Table II show that 90% of the active atoms were located in a region  $2z_2$  from the crystal edges. As was observed in the first experiment, some activity was measured in the remaining crystal, hence the strips (typically 30 to 40  $\mu\text{m}$  wide) were again cut from the crystal and the activity in these strips and the remaining crystal were measured. After the second cut no significant activity was measured in the remaining crystal, indicating that no radioactive  $^{110}\text{Ag}$  moved up to the initial stage-2 empty crystal boundary during the stage-1 to stage-2 conversion.

To confirm the results of this experiment, further experiments were done by replacing the nonactive electrolyte with the active electrolyte and vice versa. The results were consistent with those reported above.

### C. Motion of Ag perpendicular to layers of $\text{TiS}_2$

To investigate the motion of Ag along the  $c$  axis of the  $\text{TiS}_2$  crystal, as-grown crystals with thin surface steps were selected such that the thicknesses ranged from 24 to 50  $\mu\text{m}$  for the base crystal and 2.5 to 10  $\mu\text{m}$  for the steps. In these experiments only the base of the crystals were in-

tercalated with Ag (to an  $x$  value between 0.2 and 0.4) using an electrolyte of 0.1M  $\text{AgNO}_3$  in glycerol. The intercalated base crystal provided the basal plane of the unintercalated crystal step with a source of Ag. As described earlier, the crystals were scanned along a line and the distribution of Ag was determined by XRF for both the base crystal and the step. A pure  $\text{TiS}_2$  crystal was used as a reference. A 10-kV electron beam was used and at this voltage the maximum depth for detectable Ag fluorescent x rays in  $\text{TiS}_2$  was determined to be about 1  $\mu\text{m}$  from measurements on pure  $\text{TiS}_2$  crystals on a Ag substrate. Since the height of the step was greater than the maximum depth for detectable Ag fluorescent x rays, the Ag in the base crystal below the step was not detected when scanning the step. The first observations showed that Ag had not moved into the steps during the intercalation period. Observation during the following two months also gave the same result showing that the motion of Ag perpendicular to the  $\text{TiS}_2$  layers is negligible at room temperature. After heating a sample at 200°C for one day, Ag was detected in the step and the amount of Ag increased as the sample was further heated at 200°C. The diffusion coefficient for the motion of Ag perpendicular to the layers of a  $\text{TiS}_2$  crystal at 200°C was estimated using a solution to the one-dimensional diffusion equation.<sup>6</sup> The estimated diffusion coefficient is  $\sim 10^{-13}$   $\text{cm}^2/\text{sec}$  at 200°C and it is estimated to be less than  $\sim 10^{-15}$   $\text{cm}^2/\text{sec}$  at room temperature.

### III. DISCUSSION

Our results (Fig. 2) provide fairly conclusive evidence that the in-plane Ag density is constant for stage-1 and stage-2, so that there is no change in host lattice bonding energy by the stage conversion as the same number of host bonds are broken before and after the conversion. In addition, for stage-2 the Ag ion separation within a layer is the same as for stage-1 so that the Coulomb energy related to in-layer forces should be reasonably constant. However the separation of the Ag in adjacent layers for stage-2 is about twice the separation for stage-1.<sup>7</sup> Thus it appears that the driving force in the stage-1 to stage-2 conversion is the Coulomb repulsion between charged Ag ions in different layers.

With the DH model, the conversion from stage-1 to stage-2 involves the generation of bends in the host layers which costs elastic energy. Despite this, rapid conversion from stage-1 to stage-2 is observed at room temperature indicating that the elastic energy is significantly less than

TABLE II. Results of  $^{110}\text{Ag}$  tracer experiments: Stage-1 to stage-2 conversion. Crystal thickness equals 5  $\mu\text{m}$ .  $z_1$  is the width of the initial stage-2 region.  $z_2$  is the width of the  $^{110}\text{Ag}$  stage-1 region.

$z_1(\pm 5 \mu\text{m})$ $^{108}\text{Ag}$	$z_2(\pm 5 \mu\text{m})$ $^{110}\text{Ag}$	$2z_2(\pm 10 \mu\text{m})$	Whole crystal	Counts per second			
				First cut Width equals 100 $\pm$ 10 $\mu\text{m}$ Cutoff sections		Second cut Width equals 30 $\pm$ 10 $\mu\text{m}$ Cutoff sections	
				100 $\pm$ 10 $\mu\text{m}$ Remaining crystal	30 $\pm$ 10 $\mu\text{m}$ Remaining crystal		
110	40	80	11.88 $\pm$ 0.22	10.70 $\pm$ 0.22	1.17 $\pm$ 0.18	1.09 $\pm$ 0.18	0.20 $\pm$ 0.18

the decrease in the interlayer Coulomb energy. The fact that the stage-1 front remained stationary at liquid-N<sub>2</sub> temperature shows that thermal activation of the Ag atoms is required. This is also the case for the stage-2 front at room temperature as shown by the temperature dependence of stage-2 Ag in the absence of a stage-1 region in the crystal (Fig. 3).

The tracer results show that when Ag atoms enter a partially intercalated stage-2 TiS<sub>2</sub> crystal, the atoms already in the crystal are effectively pushed further into the crystal by entering Ag atoms. In addition, the tracer results show that during the conversion of stage-1 into stage-2 the Ag from stage-1 pushes the stage-2 Ag into the crystal. As mentioned earlier, the motion of Ag in the stage-2 region is probably driven by interlayer Coulomb repulsive forces between charged Ag ions in the stage-1 region.

The type of motion of stage-1 Ag into stage-2 Ag required by the tracer results can only be reasonably explained with islands of atoms within the host layers. The conversion from stage-1 to stage-2 in the classical model for staging is only possible if there is migration of Ag atoms perpendicular to the layers of the TiS<sub>2</sub> lattice and since we showed that the motion of Ag atoms perpendicular to the layers is negligible at room temperature, the classical model fails to explain the tracer results. An adaptation of the Daumas-Héroid island model to a partially intercalated crystal<sup>4</sup> can be used to explain how Ag atoms in stage-1 can remain near the crystal edge in the stage-1 to stage-2 conversion. In the model the stage-1 Ag acts as a source of moving stage-2 islands. A Coulomb repulsion between islands is required to keep the islands moving into the crystal as intercalation proceeds. Figure 2 indicates that initially there is a constant rate of generation of stage-2 islands at the stage-1 front.

In the tracer experiment which was done to study the migration of Ag in the stage-1 to stage-2 conversion, some activity was found beyond a distance from the edge greater than twice the width of the stage-1 region (Table II). This agrees with the electron microprobe XRF results where it was observed that the intercalation fronts are not sharp<sup>4</sup> and that the stage-2 front becomes wider after the conversion of stage-1 into the stage-2.

When the crystals were intercalated slowly using a low-concentration electrolyte, only stage-2 was observed both optically and by XRF measurements. It is likely that a very narrow region of stage-1 exists at the crystal edge but this may not be observable since the stage-1 rapidly converts to stage-2. Both stage-1 and stage-2 are observable if the rate of intercalation is faster than the rate of conversion of stage-1 Ag. It seems likely that it is generally true for intercalation systems that during intercalation a stage-1 is always present at the crystal edges with higher stages developing within the crystal.

It was observed that the deintercalation occurs via a stage conversion. The distribution of Ag given in Fig. 4 shows that the stage-1 to stage-2 deintercalation front is not sharp and Fig. 4 can be interpreted by the model shown in Fig. 6 (although we have no evidence, it seems likely that the depletion of Ag starts from the surface layers). In this model the stage-1 acts as the source of

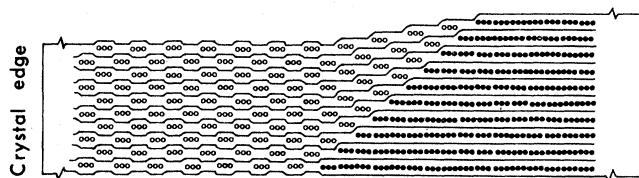


FIG. 6. Moving island model for a partially deintercalated crystal, showing only the upper half of the crystal. The lines depict the host layers. The closed circles depict regions of stage-1 Ag and the open circles depict Ag in stage-2 islands. As the crystal deintercalates, the stage-1 Ag acts as a source of moving stage-2 islands.

moving stage-2 islands. In an earlier publication<sup>4</sup> we estimated the island size to be about 130 Å for Ag in TiS<sub>2</sub>, assuming staircase or V-shaped intercalation fronts. The island width can be written as  $L = 2P/N$ , where  $N$  is the number of layers in the host crystal and  $P$  is the width of the stage-1 intercalation front. For a given thickness of the crystal,  $N$  can be calculated knowing the  $c$  lattice parameter. The same formula can be applied to the partially deintercalated crystal model of Fig. 6. Using the Ag distribution for the partially deintercalated crystal shown in Fig. 4 and the crystal thickness known to be between 0.5 and 1.0 μm, the island width formed on deintercalation is estimated to be between 100 and 200 Å. It thus appears that the Ag islands formed on intercalation and deintercalation are about the same size. As for intercalation, it appears that interlayer Coulomb repulsion is the driving force for the island formation in Fig. 6 and that Coulomb repulsion keeps the stage-2 islands moving from the stage-1 front to their demise at the edge of the crystal.

The results from Sec. II C demonstrate that the diffusion of Ag perpendicular to the layers of TiS<sub>2</sub> is negligible at room temperature. Although migration of Ag perpendicular to the layers was observed at 200°C, the estimated diffusion coefficient is still many orders of magnitude smaller than estimated room-temperature diffusion constants of  $\sim 10^{-8}$  cm<sup>2</sup>/sec for Li in TiS<sub>2</sub> (Ref. 8) and  $\sim 10^{-10}$  cm<sup>2</sup>/sec for Ag along the layers of TiS<sub>2</sub> crystals<sup>3</sup> (it has been observed that in ultrathin TiS<sub>2</sub> crystals about 300 Å thick, Ag in the stage-2 region diffuses along the layers in the absence of stage-1 Ag in the crystal<sup>3</sup>). The high anisotropy in the diffusion constant justifies the usual assumption of two-dimensional motion for Ag in TiS<sub>2</sub>. A similar anisotropy is to be expected for other intercalated dichalcogenide layer compounds.

The work described here has given us some understanding of the intercalation and deintercalation of Ag in TiS<sub>2</sub>. Further work is required to see if the models used to explain the results are applicable to other intercalation systems.

#### ACKNOWLEDGMENTS

We wish to acknowledge the considerable help of P. Joensen (including taking the data for Fig. 4) and also Dr. J. M. D'Auria of the Department of Chemistry at Simon Fraser University for his valuable assistance in the tracer experiments. The Natural Sciences and Engineering Research Council of Canada, which supported this work, is also acknowledged.

\*Permanent address: University of Sri Jayewardenepura, Nugegoda, Sri Lanka.

- <sup>1</sup>*Physics and Chemistry of Materials with Layered Structures*, edited by F. A. Lévy (Reidel, Holland, 1979), Vol. 6; M. S. Dresselhaus and G. Dresselhaus, *Adv. Phys.* **30**, 139 (1981); *Physics of Intercalation Compounds*, Vol. 38 of *Springer Series in Solid-State Sciences*, edited by L. Pietronero and E. Tosatti (Springer, Berlin, 1981).
- <sup>2</sup>N. Daumas and M. A. Hérol, *C. R. Acad. Sci. Ser. C* **268**, 373 (1963).
- <sup>3</sup>G. A. Scholz, P. Joensen, J. M. Reyes, and R. F. Frindt, *Physica* **105B**, 214 (1981).
- <sup>4</sup>D. Kaluarachchi and R. F. Frindt, *Phys. Rev. B* **28**, 3663 (1983).
- <sup>5</sup>R. O. Carlson, *J. Phys. Chem. Solids* **13**, 65 (1960).
- <sup>6</sup>H. S. Carslaw and J. C. Jaeger, *Conduction of Heat in Solids* (Oxford University Press, Oxford, 1959), p. 101.
- <sup>7</sup>G. A. Scholz and R. F. Frindt, *Mater. Res. Bull.* **15**, 1703 (1980).
- <sup>8</sup>M. S. Wittingham, *Prog. Solid State Chem.* **12**, 41 (1978).